Journal of Alloys and Compounds 527 (2012) 145–151

Contents lists available at SciVerse ScienceDirect

Journal of Alloys and Compounds

journal homepage: www.elsevier.com/locate/jallcom

# Time and temperature regime of continuous grain coarsening in an ECAP-processed Al(0.1 wt.% Sc) alloy

A. Bommareddy[a], M.Z. Quadir[a,b,*], M. Ferry[a]

[a] ARC Centre of Excellence for Design in Light Metals, School of Materials Science and Engineering, University of New South Wales, Sydney, NSW 2052, Australia
[b] Electron Microscope Unit, University of New South Wales, Sydney, NSW 2052, Australia

ARTICLE INFO

*Article history:*
Received 22 November 2011
Received in revised form 26 February 2012
Accepted 28 February 2012
Available online xxx

*Keywords:*
Aluminium alloys
Annealing
Equal channel angular pressing (ECAP)
Electron backscattering diffraction (EBSD)
Continuous recrystallization

ABSTRACT

An equiaxed, submicron grain size distribution was generated in an Al(0.1 wt.% Sc) alloy by processing through equal channel angular pressing followed by a low temperature pre-ageing heat treatment. The alloy was subsequently annealed for various times at 300, 350, 400 and 450 °C for investigating the thermal stability of the deformation microstructure. It was found that up to 400 °C, the submicron grain structure coarsens slowly and uniformly by a process of continuous recrystallization. Within this temperature range, the uniform dispersion of nano-sized $Al_3Sc$ particles generated by the pre-ageing treatment substantially hinders grain coarsening by Zener pinning of the (sub)grain boundaries. At the higher annealing temperature of 450 °C, certain grains were found to grow discontinuously thereby generating a mixed microstructure consisting of both fine and coarse grains. The data in this study was combined with recent data for a higher solute Al(0.3 wt.% Sc) alloy for furthering our understanding of the time and temperature range in which this family of alloys is resistant to rapid, discontinuous grain coarsening (recrystallization).



## 1. Introduction

Severe plastic deformation (SPD) is a contemporary approach for strengthening an alloy by refining the grain size to the submicron level. To generate this level of structural refinement, there are a number of SPD processes under intense development on a wide range of alloys, including equal channel angular pressing (ECAP) [1–7]. Here, Al alloys have received the greatest attention due to their commercial importance as lightweight materials and the technical advantages in dealing with these materials [8]. However, ECAP-processed alloys contain a high stored energy due to the high density of grain boundaries generated by the deformation and, hence, they often suffer from rapid, discontinuous grain coarsening (also known as recrystallization) at slightly elevated temperatures [9]. As a consequence, ECAP processing is problematic if elevated temperature stability of the submicron grain size is important. This problem is particularly severe in Al alloys due to the low melting temperature, as compared to other structural metals such as steels. One effective approach for preventing rapid grain coarsening after ECAP is to incorporate a distribution of ultra-fine, stable particles into the microstructure. Such particles impede grain boundary migration by Zener pinning thereby suppressing grain coarsening [10]. There are two broad approaches for generating fine particles in ECAP alloys: (i) powder processing and (ii) conventional alloy design. In the former, metal powder and particles may be mixed thoroughly together in the right proportion followed by sintering at high temperatures and high pressures [11,12]. It is pertinent to mention that a better particle compactness can also be achieved by adding right proportion of some particles, such as 10% Si–C in Al [4]. In the latter, it is possible to exploit the precipitation behaviour of certain Al alloys by adding small quantities of elements such as Sc, Si, Cu and Mg into the melt during casting [13–15]. The ECAP temperature plays a very important role in the route [6]. Scandium is known to be an effective addition to aluminium for generating a fine particle distribution during solution treatment and artificial ageing, although other rare earth elements (Hf, Zr and Er) can also form a dispersion of fine particles [16–22]. Extensive research has been carried out by Seidman's team and other researchers on the size, kinetics, chemistry and distribution of such dispersoids in aluminium when Sc was added singly or in combination with Mg, Zr and Ti [21–23], and by the current team on other SPD techniques [24,25]. The addition of small quantities of Sc to aluminium has also shown to stabilize ECAP-generated substructures at elevated temperature when fine particles are present [19,20]. More recently, Kim et al. [23] demonstrated that,

* Corresponding author at: Electron Microscope Unit, University of New South Wales, Sydney, NSW 2052, Australia.
*E-mail address:* mzquadir@unsw.edu.au (M.Z. Quadir).

0925-8388/$ – see front matter © 2012 Elsevier B.V. All rights reserved.
doi:10.1016/j.jallcom.2012.02.181

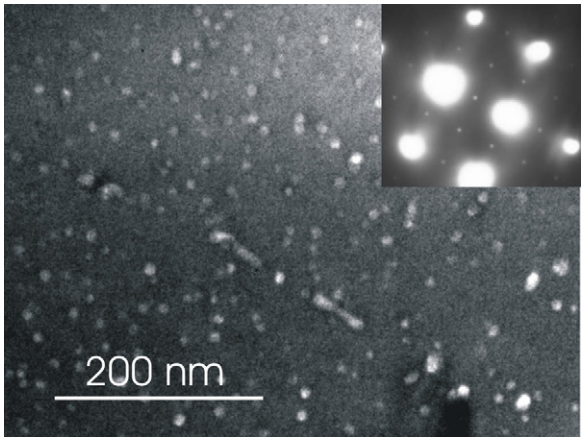


**Fig. 1.** Dark field TEM micrograph and corresponding selected area diffraction pattern showing the dispersion of $Al_3Sc$ precipitates after pre-ageing for 30 h at 250 °C.

the ECAP processing and aging sequence (as low as at 100 °C) has significant influences in their strain harden ability. This finding implies that the form of Sc (solute atom or particles) is important in determining their deformation behaviour [23]. In another SPD technique, by rolling, the effectiveness of Sc (either in the form of solute and particles) for enhancing fragmentation and preventing recrystallization was demonstrated by Quadir et al. [24,25].

Ferry and Burhan [20] recently carried out a statistical analysis of the effectiveness of 0.3 wt.% Sc addition to Al on maintaining an ultra-fine grain structure after ECAP and subsequent annealing at high temperature. It was found that, after ECAP, the generation of a uniform distribution of nano-sized $Al_3Sc$ particles throughout the Al matrix by a pre-ageing treatment resulted in very slow and homogenous grain coarsening at temperatures up to 500 °C by a mechanism known as continuous recrystallization (or continuous subgrain growth). They also noted that, while the highly strained ECAP microstructures generally contain a non-uniform distribution of boundary type (low and high angle boundaries), the simple low temperature pre-aging treatment was sufficient to maintain an ultra-fine and homogeneous grain size distribution during annealing at temperatures up to 500 °C. A detailed statistical analysis of grain coarsening of this Al(0.3)Sc alloy showed that the stabilized microstructure maintains a lognormal grain size distribution in the continuous coarsening regime. It is pertinent to note that the alloying processes with higher scandium contents are expensive [8]. Hence, it was deemed necessary to investigate the influence of much lower concentrations of Sc on the grain coarsening behaviour of these submicron grain structures. In the present study, we investigate the grain coarsening behaviour in a low solute (Al(0.1% Sc)) alloy; this scandium concentration is just above the solid solution limit for generating $Al_3Sc$ particles during pre-ageing. The performance of this concentration in terms of the high temperature stability of submicron structures is also scientifically important as it was shown by Seidman et al. [21,22] that the number density of the $Al_3Sc$ particles after artificial ageing of (Al(0.1% Sc)) is considerably less than that generated in Al(0.3% Sc). The effectiveness of the particles in preventing the substructure from coarsening is not evaluated for this alloy system, and this is the aim of the present paper.

## 2. Experimental procedures

A high purity Al(0.1% Sc) alloy was gravity chill cast to produce 15 mm diameter ingots and then swaged to 10 mm diameter rods. The alloy composition was confirmed by Inductively Coupled Plasma (ICP) analysis to be within ±8% of the target value. The rods were then solution heat treated above the solvus for 48 h at 620 °C and then room temperature water quenched. The sample was investigated by transmission electron microscopy (TEM) following an ageing treatment for 30 h at 250 °C to confirm that nano-sized (<10 nm) $Al_3Sc$ particles are generated. Indeed, the dark field TEM micrograph in Fig. 1 shows that the particles are nano-sized, spherical and dispersed uniformly. The diffraction pattern (inset in Fig. 1) shows the relevant spots from both the $Al_3Sc$ particles and matrix. Following confirmation that fine $Al_3Sc$ particles are generated in this alloy, samples of 10 mm diameter and 100 mm length were solution treated at 620 °C and deformed by ECAP at room temperature to an equivalent von Mises strain of 9.2. The ECAP rig had characteristic angles $\Phi = 90°$ and $\Psi = 0$ and pressing was carried out using graphite lubricant at a ram speed of 10 mm/min to a total of 8 passes with 90° rotation between passes. Following ECAP, the alloy was pre-aged for 30 h at 250 °C to produce a submicron, equiaxed microstructure containing coherent $Al_3Sc$ particles. The samples were then annealed for up to 10 h at 300, 350, 400 and 450 °C. Similar to the previous study on an Al(0.3% Sc) alloy [20], grain coarsening was investigated by focused ion beam (FIB) microscopy, field emission gun scanning electron microscopy (FEGSEM) and electron back scatter diffraction (EBSD).

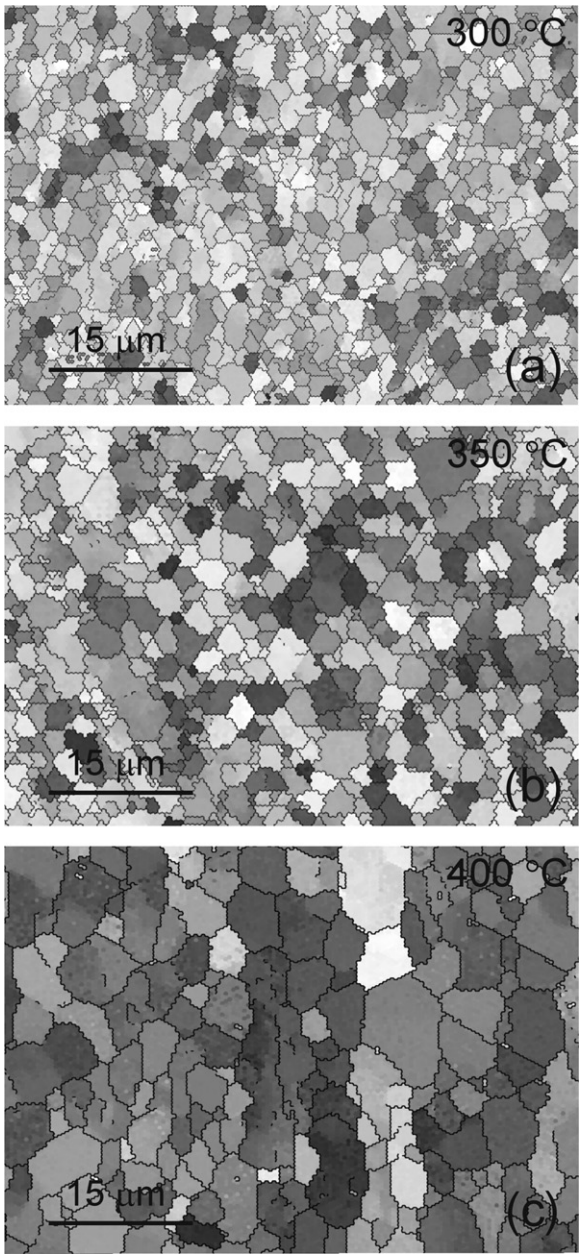


**Fig. 2.** EBSD micrographs showing the grain distributions after annealing for 10 h at 300, 350 and 400 °C. Black lines represent >7° misorientation boundaries.

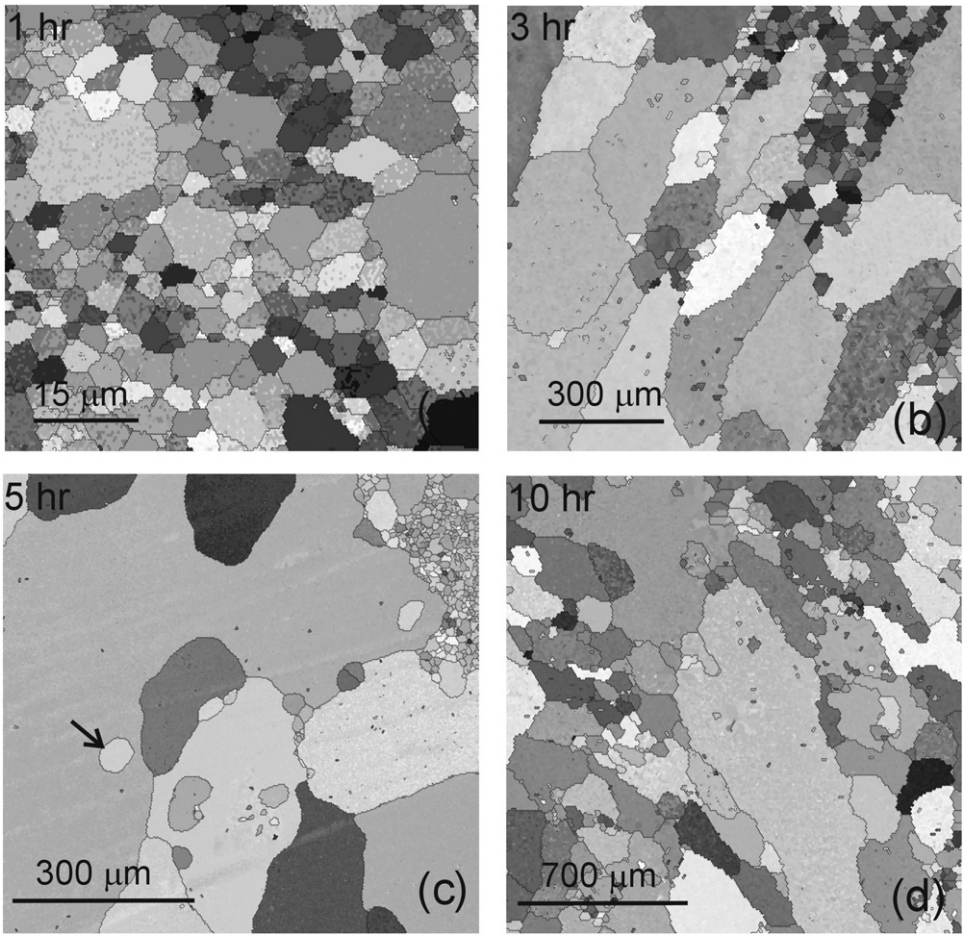


**Fig. 3.** EBSD micrographs showing the grain distributions after annealing for 1, 3, 5 and 10 h at 450 °C. Black lines represent >15° misorientation boundaries.

## 3. Results and discussion

### 3.1. Microstructural evolution during pre-ageing and annealing

After 30 h pre-ageing at 250 °C, an equiaxed subgrain microstructure (0.90 μm mean diameter) was generated. This grain structure was deemed to be stable since longer ageing times did not cause any significant changes to the microstructure. Within each grain, the orientation was constant thereby indicating that substantial recovery had occurred during pre-ageing. Isothermal annealing was carried out for 1, 3, 5 and 10 h at a given temperature (300, 350, 400 and 450 °C) where it was found that coarsening was gradual (and uniform) at temperatures below 450 °C. For example, the starting grain diameter of 0.90 μm increased to only 1.62 μm after annealing for 10 h at 300 °C. Fig. 2 shows EBSD micrographs of samples annealed for 10 h at 300, 350 and 400 °C showing uniform grain coarsening. Annealing also retained a large fraction of high angle grain boundaries (HAGBs) with only a small fraction of low angle (5–15°) grain boundaries (LAGBs). The type of grain coarsening observed up to 400 °C in this alloy is characterized as continuous recrystallization [19].

During annealing at 450 °C, the microstructure was no longer stable and rapid coarsening of certain grains was observed. Fig. 3 shows a series of EBSD micrographs revealing the non-uniformity in grain coarsening. After 1 h (Fig. 3a), a few grains have started growing preferentially and, after longer times, both fine (<20 μm) and coarse (>500 μm) grains are distributed throughout the microstructures (Fig. 3b–d). The discontinuous coarsening also generated small grains trapped within larger grains, as shown by the arrow in Fig. 3c. These island-type grains are similar to those observed in many Al- and Fe-based alloys when extensive growth of a small number grains occurs [20], and are argued to form as a result of the differences in growth rate between boundaries.

### 3.2. Statistical analysis of grain size distributions during coarsening

For a given annealing condition, the grain size distribution was determined from the EBSD data, which were acquired from random locations on the samples for ensuring statistical validation. The data are summarized in Table 1, which also includes the maximum grain diameter for a given annealing condition. Table 1 also provides the ratio of the maximum grain diameter to the corresponding mean diameter ($D_{max}/\bar{D}$), where it can be seen that this value remains below 2.5 for all annealing conditions except for 3 h or longer at 450 °C where it increases to above 40. This clearly indicates that discontinuous grain coarsening commences at the critical temperature of 450 °C. The results given in Table 1 clearly demonstrate that only 0.1% Sc in aluminium, in conjunction with an initial pre-ageing treatment, is sufficient to maintain a stable submicron structure at temperatures up to 400 °C.

To gain a more fundamental understanding of the normal subgrain/grain coarsening behaviour in polycrystalline materials, a number of continuous probability distributions, such as the lognormal, Rayleigh and Gamma distributions, have been compared with experimentally measured grain size data. The recent grain coarsening study by Ferry and Burhan [20] on their higher solute Al(0.3% Sc) alloy showed that the lognormal distribution was the best fit

**Table 1**
Measured and calculated grain size parameters, and computed $Al_3Sc$ particle parameters after annealing at various times and temperatures.

| Annealing temperature (°C) | Time (h) | Mean diameter ($\bar{D}$, μm) | $D_{max}/\bar{D}$ | Standard deviation ($\sigma$) | $\tilde{\mu}$ | $\tilde{\sigma}$ | Particle volume fraction ($f$) | Particle diameter ($d$) nm |
|---|---|---|---|---|---|---|---|---|
| 250 (pre-ageing) | 30 | 0.90 | 1.55 | 0.19 | 0.12 | 0.22 | | |
| 300 | 1 | 1.01 | 2.15 | 0.31 | 0.03 | 0.29 | 0.0039 | 5 |
| | 3 | 1.40 | 1.75 | 0.39 | 0.30 | 0.28 | | 5 |
| | 5 | 1.49 | 1.79 | 0.41 | 0.29 | 0.29 | | 5 |
| | 10 | 1.62 | 2.00 | 0.47 | 0.44 | 0.28 | | 5 |
| 350 | 1 | 1.41 | 2.17 | 0.44 | 0.30 | 0.30 | 0.0038 | 5 |
| | 3 | 1.65 | 2.20 | 0.57 | 0.44 | 0.35 | | 5 |
| | 5 | 1.72 | 2.29 | 0.66 | 0.48 | 0.35 | | 5 |
| | 10 | 2.17 | 1.99 | 0.66 | 0.72 | 0.31 | | 6 |
| 400 | 1 | 1.64 | 1.98 | 0.43 | 0.64 | 0.32 | 0.0036 | 7 |
| | 3 | 1.99 | 1.78 | 0.59 | 0.46 | 0.26 | | 10 |
| | 5 | 2.14 | 1.98 | 0.67 | 0.66 | 0.30 | | 11 |
| | 10 | 3.07 | 2.16 | 1.04 | 1.06 | 0.32 | | 14 |
| 450 | 1 | 4.03 | 1.96 | 1.41 | 1.33 | 0.33 | 0.0032 | 17 |
| | 3 | 8.01 | 39.9 | 3.45 | – | – | | 25 |
| | 5 | 10.02 | 49.9 | 4.12 | – | – | | – |

of their data for a wide range of annealing conditions. A rigorous analysis of grain coarsening in the Al(01.% Sc) alloy also revealed that the lognormal distribution is the best fit of the data [26]. The calculation method for generating this lognormal distribution from the experimental data is described in detail in Ref. [20] and given in Appendix 1. The grain size frequency histogram after pre-ageing for 30 h at 250 °C is given in Fig. 4a which reveals the small spread in grain diameter and a maximum diameter of 1.4 μm. Superimposed on this histogram is the theoretical lognormal distribution that illustrates the very close fit of the data. Fig. 4b and c shows a series of lognormal grain size distributions fitted to the experimental grain size data showing that an increase in either annealing time or temperature causes an increase in the mean diameter, a decrease in peak frequency and a broadening of the size distribution. It was shown that the lognormal distribution remains a good fit for the data even after 10 h at 400 °C [26], thereby confirming the uniformity of the coarsening observed in the EBSD micrographs (Fig. 2). After 1 h at 450 °C, there is a deviation from lognormality due to the rapid growth of certain grains within the fine-grained matrix (Fig. 3a). However, a separate plot of the data taken exclusively within these fine-grained regions confirmed that a lognormal distribution remains valid (not shown). This indicates that, despite the commencement of discontinuous grain coarsening, much of the deformation substructure continues to coarsen in a continuous manner.

A rigorous statistical analysis of the entire dataset is possible by comparing the arithmetic mean grain size ($\bar{D}$) and standard deviation ($\sigma$) of the experimentally measured data set with the computed values ($\overline{D_C}$ and $\sigma_C$) generated from the fitted lognormal distributions. Both $\overline{D_C}$ and $\sigma_C$ are related to $\tilde{\mu}$ and $\tilde{\sigma}$ by the following relations [20]:

$$\overline{D_C} = \exp\left(\tilde{\mu} + \frac{\tilde{\sigma}^2}{2}\right) \quad (1)$$

$$\sigma_C = \sqrt{\exp(2\tilde{\mu} + \tilde{\sigma}^2)(\exp(\tilde{\sigma}^2) - 1)} \quad (2)$$

Table 1 includes these computed values for all annealing conditions with Fig. 5 showing the relationship between the experimental and computed values of the mean diameter and standard deviation, respectively. For completeness, Fig. 5 includes the data for the Al(0.3% Sc) alloy [20]. The computed statistical parameters correspond closely with the measured values for a wide range of annealing conditions although, for both alloys, the open symbols reveal the marked variation from lognormality due to the onset of discontinuous grain coarsening. It is pertinent to

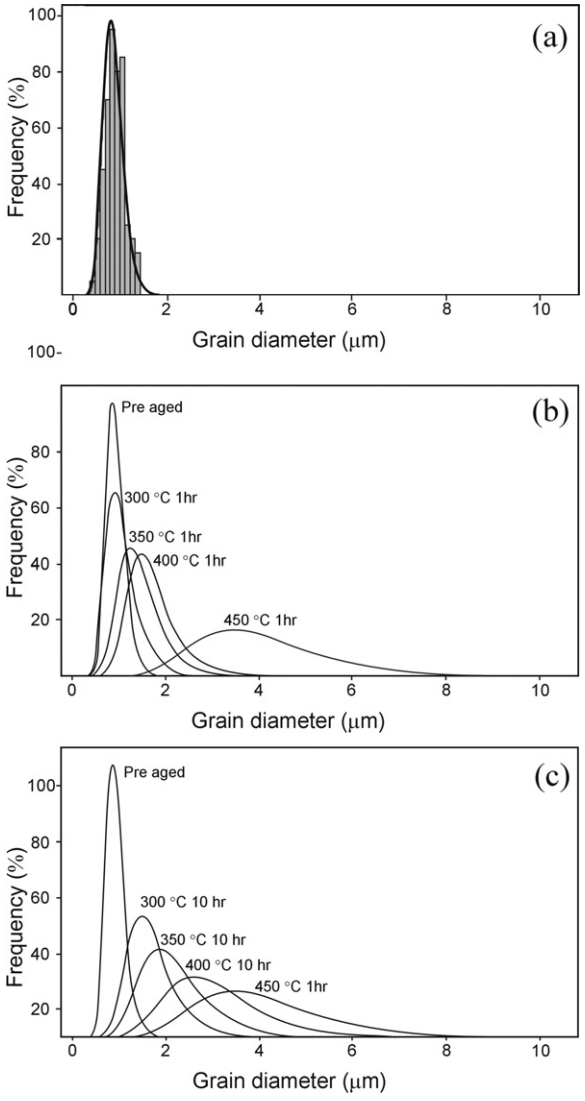


**Fig. 4.** (a) Grain size frequency histogram after pre-ageing for 30 h at 250 °C including the superimposed lognormal probability distribution which was the best fit of the data. Fitted lognormal grain size distributions after annealing for (b) 1 h and (c) 10 h at various temperatures showing the broadening of the size distributions during extended annealing. The data for 1 h annealing at 450 °C is included for comparison.

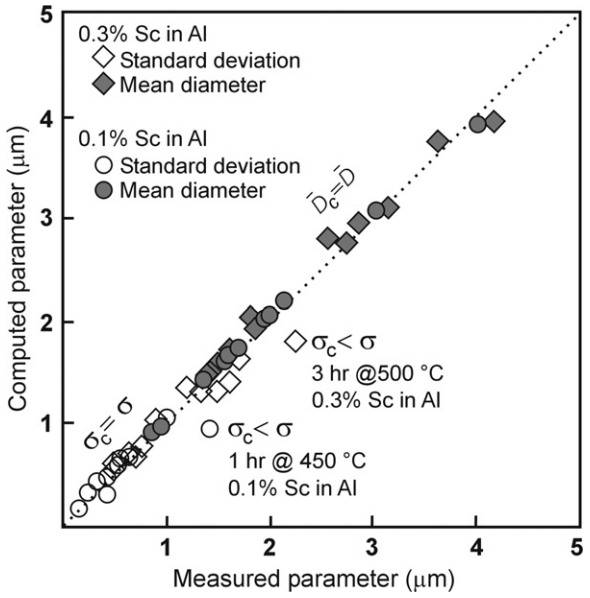


**Fig. 5.** Relationship between the measured arithmetic mean grain size and standard deviation with the calculated parameters generated from the fitted lognormal distributions, for isothermal annealing for 1–10 h at 300–400 °C and 1 h at 450 °C. Data for an Al(0.3% Sc) alloy from Ref. [15] are included to represent the time–temperature space of this alloy system.

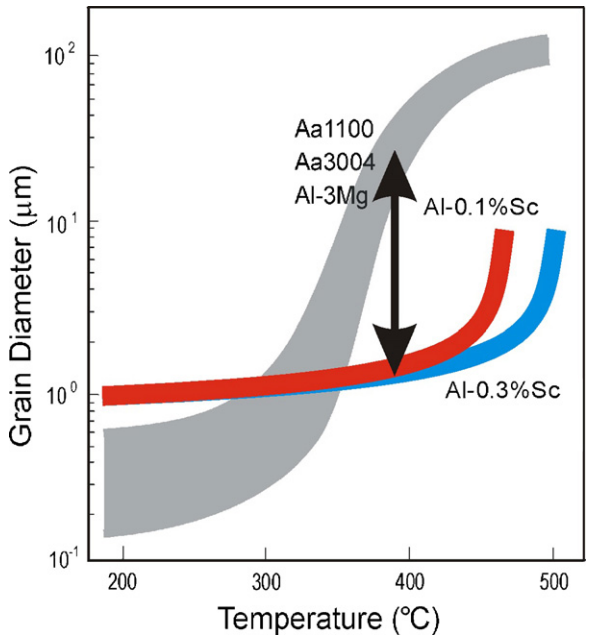


**Fig. 6.** Grain diameter as a function of annealing temperature (1 h and 2 h annealing at a given temperature) for various commercial Al alloys produced by ECAP [26] and the Al(0.1% Sc) and Al(0.3% Sc) [15] alloys.

note that this phenomenon commences in the Al(0.1% Sc) alloy at a shorter time and lower temperature than the Al(0.3% Sc) alloy. Therefore, the number density of $Al_3Sc$ particles in the Al matrix, which is governed by scandium concentration, appears to have a substantial influence on the onset of discontinuous grain coarsening in this binary alloy system.

### 3.3. *Influence of the $Al_3Sc$ particles on the transition from continuous to discontinuous grain coarsening*

Particle-free alloys exhibiting a submicron grain size are generally unstable at high temperatures due to the high stored energy associated with the large surface area of grain boundaries in a given volume of material [27]. Hence, annealing at moderate temperatures (300–350 °C) is sufficient to cause rapid grain coarsening in these alloys. Fig. 6 is a schematic diagram illustrating the general stability of the Al(0.1% Sc) and Al(0.3% Sc) alloys in comparison with other submicron grain size Al alloys produced by ECAP. The average grain sizes in these alloys were generated by isochronal annealing (1–2 h at a given temperature) and the details are provided in Ref. [26]. It is clear that, while the Al alloy studied herein contains only a small amount of scandium, it is considerably more resistant to grain coarsening compared with Al alloys not containing fine particles. Indeed, the present low-solute alloy is almost as resistant to grain coarsening as the Al(0.3% Sc) alloy.

For conventional particle-containing alloys containing a grain size greater than a micron, discontinuous recrystallization is prevented when the particle dispersion parameter ($f/d$) is greater than 0.1 μm [27], where $f$ and $d$ is the volume fraction and mean particle diameter, respectively. However, it is possible that a much larger $f/d$-value is needed for preventing recrystallization in submicron microstructures [27–29] (i.e. $f/d \sim 1.5/\mu m$ for 0.5 μm grain size [28]). It is therefore useful to determine the critical $f/d$-value associated with discontinuous grain coarsening in the present alloy. We can estimate this parameter using data for coarsening behaviour of $Al_3Sc$ particles in a submicron grained Al(0.2% Sc) alloy [19], which was shown to correspond to the classic Lifshitz–Slyozov–Wagner (LSW) theory of particle coarsening [30,31]:

$$d = \left( d_o^3 + \frac{8c_\alpha(1-c_\alpha)\gamma V_m D_o \exp(-Q_b/RT)t}{9RT(c_\beta - c_\alpha)^2} \right)^{1/3} \quad (3)$$

where $d_o$ is the particle diameter of the pre-aged alloy ($\sim 5 \times 10^{-9}$ m [26]), $d$ the average particle diameter at time, $t$, $V_m$ the partial molar volume of Sc in $Al_3Sc$ (=$1.035 \times 10^{-3}$ $m^3$/mol [32]), $\gamma$ the interfacial free energy between the Al matrix and $Al_3Sc$ (=0.2 $J/m^2$), $D_o = 5.31 \times 10^{-4}$ $m^2/s$ [33] and $Q_b$ the activation energy for bulk diffusion of Sc atoms in Al (=173 kJ/mol) [33]. $c_\alpha$ and $c_\beta$ (=25 at.%) is the equilibrium concentration of Sc in the Al matrix and $Al_3Sc$, respectively, with the former given as [33]:

$$c_\alpha = \exp\left(\frac{\Delta S}{R}\right) \cdot \exp\left(\frac{-\Delta H}{RT}\right) \quad (4)$$

where $\Delta S/R$ is a constant (=6.57) and $\Delta H$ is the enthalpy change (=62.8 kJ/mol) for dissolving Sc in the Al matrix.

A reasonable estimate of the $Al_3Sc$ particle volume fraction, $f$, may be obtained from the equilibrium lever rule [19]:

$$f = \frac{c_o - c_\alpha}{c_\beta - c_\alpha} \quad (5)$$

The computed particle parameters for the Al(0.1% Sc) alloy are included in Table 1. Since $D_{max}/\bar{D} > 3$ is a useful indicator of a microstructure undergoing a discontinuous coarsening process (i.e. recrystallization) [27], $D_{max}/\bar{D}$ is plotted as a function of $f/d$ in Fig. 7 for both Al(0.1% Sc) and Al(0.3% Sc) [34]. It is clear that the alloys begin to recrystallize when $f/d \sim < 0.5/\mu m$, where the mean grain diameter of the surrounding microstructure is a few microns. Hence, this transition in coarsening behaviour occurs when the alloys are no longer ultra-fine-grained, i.e. the critical $f/d$-value for 'recrystallization' falls between the values computed for submicron grained alloys [28] and that observed for conventionally deformed alloys [27]. It is pertinent to note that the Al(0.1% Sc) alloy undergoes discontinuous grain coarsening at a lower temperature than the Al(0.3% Sc) alloy (Fig. 6). This is likely to be related to the difference in $f/d$-values for a given annealing condition. For a range of

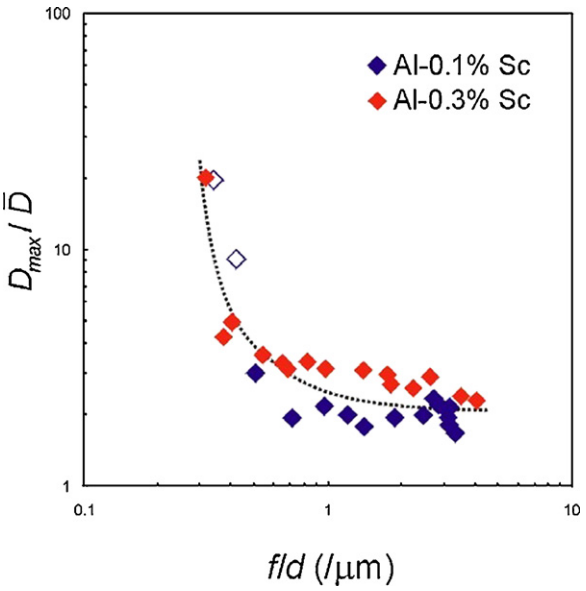


**Fig. 7.** The ratio of maximum to mean grain diameter ($D_{max}/\bar{D}$) as a function of the particle dispersion parameter ($f/d$) for the Al(0.1% Sc) and Al(0.3% Sc) [26] alloys (open symbols are estimated grain size values taken from ICC micrographs).

Al–Sc alloys (0.06–0.4% Sc) [35,36], it was shown that an increase in scandium content increases the $Al_3Sc$ particle density ($f$) without altering their size ($d$), for a given annealing condition. This observation implies that the $Al_3Sc$ particle density (volume fraction) in the submicron Al–Sc alloys is the principal factor controlling discontinuous grain coarsening. Therefore, the particle coarsening at higher temperatures will reduce their number density and eventually lead to discontinuous coarsening, although the detailed mechanism of the process is not fully understood [19].

## 4. Conclusions

An Al(0.1% Sc) alloy was deformed by ECAP and pre-aged for 30 h at 250 °C to produce a submicron grain size consisting of a lognormal distribution. A statistical analysis of the EBSD data shows that this alloy is highly resistant to both continuous and discontinuous grain coarsening during extended annealing at temperatures up to 450 °C. Here, the grain diameter increases slightly during annealing and the size distribution remains lognormal. However, annealing at 450 °C results in discontinuous grain coarsening (recrystallization) whereby certain grains grow rapidly by consuming the surrounding fine-grained microstructure. The general coarsening behaviour of the Al(0.1% Sc) alloy is similar to that observed in a higher solute Al(0.3% Sc) alloy, although the latter is resistant to discontinuous coarsening at higher temperatures (500 °C). The only major difference appears to be the lower $Al_3Sc$ particle density in the Al(0.1% Sc) alloy thereby slightly reducing the temperature at which discontinuous grain coarsening commences. The results also confirm that that a very low scandium concentration in aluminium is adequate for retaining an ultra-fine-grained microstructure at elevated temperature.

## Appendix 1.

The arithmetic mean grain size ($\bar{D}$) and standard deviation ($\sigma$) were calculated from the following:

$$\bar{D} = \frac{\sum N_i D_i}{\sum N_i} \tag{A1}$$

$$\sigma = \left[\frac{\sum N_i (D_i - \bar{D})^2}{\sum N_i}\right]^{1/2} \tag{A2}$$

where $N_i$ is the given number of grain diameter $D_i$.

To generate a lognormal distribution on the frequency histogram of the given population of grains, it is necessary to calculate in logarithmic values:

$$\ln(D_i) \sim N(\mu, \sigma) \tag{A3}$$

In Eq. (A3), $N$ is normal with two parameters; by convention, $D_i$ is called a lognormal random variable because its logarithmic follows the normal distribution. The parameters $\tilde{\mu}$ and $\tilde{\sigma}$ are calculated from Eqs. (4) and (5):

$$\tilde{\mu} = \frac{\sum (N_i \ln D_i)}{\sum N_i} \tag{A4}$$

$$\tilde{\sigma} = \sqrt{\frac{\sum N_i (\ln D_i - \tilde{\mu})^2}{\sum N_i}} \tag{A5}$$

The lognormal probability distribution function is followed by these two parameters $\tilde{\mu}$ and $\tilde{\sigma}$, whereby the formula is given as:

$$P(D) = \frac{1}{\sqrt{2\pi}\tilde{\sigma} Di} \exp\left[-\frac{1}{2}\left(\frac{\ln D_i - \tilde{\mu}}{\tilde{\sigma}}\right)\right], \quad D_i > 0 \tag{A6}$$

From Eq. (A6), it is possible to calculate the lognormal distribution for a given grain size frequency histogram.

## Appendix B. Supplementary data

Supplementary data associated with this article can be found, in the online version, at doi:10.1016/j.jallcom.2012.02.181.

## References

[1] R.Z. Valiev, R.K. Islamgaliev, I.V. Alexandrov, Prog. Mater. Sci. 45 (2000) 103–189.
[2] R.Z. Valiev, T.G. Langdon, Prog. Mater. Sci. 51 (2006) 881–981.
[3] C.M. Cepeda-Jiménez, J.M. García-Infanta, O.A. Ruano, F. Carreño, J. Alloys Compd. 509 (2011) 9589–9597.
[4] B. Mani, M.H. Paydar, J. Alloys Compd. 492 (2010) 116–121.
[5] M. Wang, A. Shan, J. Alloys Compd. 455 (2008) L10–L14.
[6] P. Málek, M. Cieslar, R.K. Islamgaliev, J. Alloys Compd. 378 (2004) 237–241.
[7] S.Z. Hana, M. Goto, C. Lima, C.J. Kima, S. Kimc, J. Alloys Compd. 434–435 (2007) 304–306.
[8] I. Polmear, Light Alloys, 4th edition, Elsevier, 2006.
[9] J.H. Driver, Scr. Mater. 51 (2004) 819–823.
[10] P.A. Manohar, M. Ferry, T. Chandra, ISIJ Int. 38 (1998) 913–924.
[11] A.V. Korznikov, I.M. Safarov, D.V. Laptionok, R.Z. Valiev, Acta Metall. Mater. 39 (1991) 3193–3197.
[12] W. Xu, X. Wu, T. Honma, S.P. Ringer, K. Xia, Acta Mater. 57 (2009) 4321–4330.
[13] M. Asta, V. Ozolins, C. Woodward, JOM 53 (2001) 16–19.
[14] J. Grobner, R. Schmid-Fetzer, A. Pisch, G. Cacciamani, P. Riani, N. Parodi, Z. Metallkd. 90 (1999) 11.
[15] S.P. Ringer, K. Hono, Mater. Charact. 44 (2000) 101–131.
[16] H. Hallem, B. Forbord, K. Marthinsen, Mater. Sci. Eng. A 387–389 (2004) 940–943.
[17] K. Ihara, Y. Miura, Mater. Sci. Eng. A 387–389 (2004) 647–650.
[18] A. Inoue, H. Kimura, Mater. Sci. Eng. A 286 (2000) 1–10.
[19] M. Ferry, N.E. Hamilton, F.J. Humphreys, Acta Mater. 53 (2005) 1097–1109.
[20] M. Ferry, N. Burhan, Acta Mater. 55 (2007) 3479–3491.
[21] K.E. Knipling, R.A. Karnesky, C.P. Lee, D.C. Dunand, D.N. Seidman, Acta Mater. 58 (2010) 5184–5195.
[22] C.B. Fuller, D.N. Seidman, Acta Mater. 53 (2005) 5415–5428.
[23] W.J. Kim, J.K. Kim, H.K. Kim, J.W. Park, Y.H. Jeong, J. Alloys Compd. 450 (2008) 222–228.
[24] M.Z. Quadir, M. Ferry, O. Al-Buhamad, P.R. Munroe, Acta Mater. 57 (2009) 29–40.
[25] M.Z. Quadir, O. Al-Buhamad, L. Bassman, M. Ferry, Acta Mater. 55 (2007) 5438–5448.
[26] A. Bommareddy, Thermal stability of a submicron grain structure in an Al–Sc alloy, M.Sc. Thesis, University of New South Wales, 2008.
[27] F.J. Humphreys, M. Hatherly, Recrystallization Related Annealing Phenomena, second edition, Elsevier Ltd., Oxford, UK, 2004.

[28] F.J. Humphreys, P.B. Prangnell, J.R. Bowen, A. Gholinia, C. Harris, Philos. Trans. A 357 (1999) 1663–1680.
[29] F.J. Humphreys, Acta Mater. 45 (1997) 4231–4240.
[30] I.M. Litshitz, V.V. Slyozov, J. Phys. Chem. Solids 19 (1961) 35–50.
[31] C.Z. Wagner, Electrochemistry 65 (1961) 581–591.
[32] S. Fujikawa, Defect Diffus. Forum 114 (1997) 143–147.
[33] H.H. Jo, S. Fujikawa, Mater. Sci. Eng. A 171 (1993) 151–161.
[34] M. Ferry, N. Burhan, Scr. Mater. 56 (2007) 525–528.
[35] E.A. Marquis, D.N. Seidman, Acta Mater. 53 (2005) 4259–4268.
[36] M.E. van Dalen, D.C. Dunand, D.N. Seidman, Acta Mater. 53 (2005) 4225–4235.